HOKKAIDO UNIVERSITY

Title	Visualization of sucrose distribution biosynthesized in vitro from external [1-13C]sorbitol in apple (Malus domestica) fruit utilizing MALDI-TOF MSI
Author(s)	Yamashita, Ruka; Fujiki, Takumi; Horikawa, Kentaro et al.
Citation	Food Chemistry, 469 https://doi.org/10.1016/j.foodchem.2024.142545
Issue Date	2024-12-18
Doc URL	https://hdl.handle.net/2115/97381
Rights(URL)	https://creativecommons.org/licenses/by-nc-nd/4.0/
Type	journal article
File Information	oodchem_469_142545.pdf

Hokkaido University Collection of Scholarly and Academic Papers : HUSCAP

Visualization of sucrose distribution biosynthesized *in vitro* from external [1-^{13}C]sorbitol in apple (*Malus domestica*) fruit utilizing MALDI–TOF MSI

Ruka Yamashita[1], Takumi Fujiki[1], Kentaro Horikawa[2], Yutaka Jitsuyama[1], Jun Kasuga[3], Keiji Ueno[4] and Takashi Suzuki[1*]

[1] *Research Faculty and Graduate School of Agriculture, Hokkaido University, Sapporo, 060-8589, Japan*

[2] *Kamikawa Agricultural Experiment Station, Hokkaido Research Organization, Pippu, 078–0397, Japan*

[3] *Research Center for Global Agromedicine, Obihiro University of Agriculture and Veterinary Medicine, Obihiro, 080-8555, Japan*

[4] *Graduate School of Dairy Science, Rakuno Gakuen University, Ebetsu, 069-8501, Japan*

Corresponding author at: Research Faculty and Graduate School of Agriculture, Hokkaido University, Sapporo, Hokkaido 060-8589, Japan.

E-mail address: suz-tak@agr.hokudai.ac.jp (T. Suzuki).

Phone/FAX: +81 11 706 4937

Abstract

To clarify the cause of graded distribution of sucrose in apple fruit flesh, a quarter cut of young apple fruit was cultured for 72 h on agar-solidified MS medium supplemented with 0.5 M [1-^{13}C]sorbitol, with the longitudinal or horizontal cut face being attached with the medium, and distribution of ^{13}C-labelled sucrose in a specimen obtained by slicing the fruit along with the cut face was visualized utilizing MALDI–TOF MSI. Heat map images on the distribution of the peaks of sorbitol containing ^{13}C-atom indicated that external [1-^{13}C]sorbitol had penetrated evenly into the tissue. In addition, the fact that a graded increase in the content of sucrose containing ^{13}C-atom in a molecule was confirmed from the center to the outer areas of the fruit, indicates that sucrose biosynthetic ability might be higher at the cortex side of the receptacle than at the pith side in the fruit flesh.

Keywords

Fruit flesh, HPLC, receptacle, soluble carbohydrates, stable isotope, tissue culture.

1. Introduction

The taste and functions of fruits and vegetables as foods can be affected by the distribution of phytochemicals in the tissues. In a previous experiment on visualizing localization of soluble carbohydrates in a horizontal section of mature apple fruit flesh utilizing Matrix-assisted laser desorption/ionization time-of-flight mass spectrometry imaging (MALDI-TOF MSI), it was demonstrated that sorbitol localized at the center of the fruit, but the concentration of sucrose increased gradually from the center to the cortex side of the receptacle (Horikawa et al., 2019). Sucrose and sorbitol play an important roles in sugar metabolism and the sweetness of the mature apple fruits, and thus distribution of these soluble carbohydrates in the fruit may affect the taste (Li et al., 2018, Aprea et al., 2020). It is commonly known that sucrose could be biosynthesized in apple fruit tissue through several biosynthetic pathways from sorbitol (Fig. 1), which has been translocated into the fruit via pedicel (Yamaki & Ishikawa, 1986, Gao et al., 2005). Sorbitol is introduced into cytoplasm via sorbitol-transporter (Yamaki, 2010, Yuan et al., 2023), then converted into fructose and glucose by two independent reactions catalyzed by NAD–dependent sorbitol dehydrogenase (NAD–SDH) and NADP–dependent sorbitol oxidase (NADP–SOD), respectively (Loescher et al., 1982, Yamaki, 1984). Sucrose is biosynthesized in the cells from UDP–glucose and fructose–6–phosphate in a sequence of two reactions catalyzed by sucrose phosphate synthase (SPS, EC 2.4.1.14) and sucrose phosphate phosphatase (SPP, EC 3.1.3.24) (Li et al., 2012). Alternatively, sucrose may be biosynthesized from UDP–glucose and fructose in a reversible reaction catalyzed by sucrose synthase (SuSy, EC 2.4.1.13). Furthermore, sucrose can easily be broken down into glucose and fructose in a reaction catalyzed by invertase (EC 3.2.1.26). However, the reason why localization of sorbitol occurs at the center of the fruit and why gradation of sucrose concentration in the fruit flesh has been formed has not yet been clarified.

66 The use of a stable isotope like ^{13}C, which is harmless to humans, is safe and
67 available not only for tracing a molecule which was taken up and translocated from the
68 treated point on a plant (Sha et al., 2020), but also for estimating biosynthetic reaction
69 from a substrate to products in a plant tissue (Suzuki et al., 2013). In the latter case, it
70 was clearly demonstrated that short chain fructo-oligosaccharides had been
71 biosynthesized from external [1-^{13}C]glucose in asparagus stem tissue during 72 h of
72 culture utilizing MALDI-TOF MS and ESI-MS. Furthermore, the presence of a
73 significant amount of sucrose molecules which had 1 and 2 heavier *m/z* values than
74 that of naturally occurring sucrose was also confirmed. This fact indicates that they
75 might also be biosynthesized from external [1-^{13}C]glucose. Since their peaks in the
76 mass spectrum were independently separated from the peak of naturally occurred
77 sucrose (without ^{13}C), it seems possible to visualize the distribution of sucrose which
78 had been biosynthesized from the external substrate labelled with ^{13}C using
79 MALDI-TOF MSI. The availability of utilizing stable isotopes combined with
80 MALDI-TOF MSI was reported in such a case as quantifying candesartan in the tissue
81 sections cut from kidney and blood vessels of mice (Nakanishi et al., 2013). Studies
82 using MALDI-TOF MSI have also been increasing in the field of plant science (Kaspar
83 et al, 2011, Yoshimura et al., 2012, Franceschi et al, 2012, Feenstra et al., 2017,
84 Enomoto et al., 2018, Fujita et al., 2019, Wang et al., 2021, Lu et al., 2023).
85 This study was designed to investigate locational differences of sucrose biosynthetic
86 activity in apple fruit flesh by culturing fruit cuts for 72 h on agar-solidified medium
87 supplemented with a high concentration of [1-^{13}C]sorbitol as a substrate, and then
88 visualizing the distribution of ^{13}C-labelled sucrose in the longitudinal and horizontal
89 sections of the fruit utilizing MALDI–TOF MSI.
90

91 **2. Materials and methods**

92 *2.1. Plant materials and reagents*

93 Apple fruits (*Malus domestica* cv. Kotoku), 40-45 mm in diameter, were collected on
94 26 July, 2021 (75 days after bloom), from a 35-year-old tree grown in the experimental
95 orchard of Hokkaido University in Yoichi, Japan. A special grade of methanol and an
96 HPLC grade of acetonitrile were purchased from Kanto Chemical Co. Inc. (Tokyo,
97 Japan). A special grade of standard fructose, sorbitol, glucose and sucrose were
98 purchased from Nacalai tesque Inc. (Kyoto, Japan). As a reagent labelled with a stable
99 isotope, [1-^{13}C]D-sorbitol (99% in purity) was purchased from Cambridge Isotope Lab.
100 Inc. (Andover, MA, USA). As a matrix for MALDI–TOF MSI, 2,5-dihydroxybenzoic
101 acid (DHB) was purchased from the Wako Pure Chemical Industries Ltd. (Osaka,
102 Japan).
103
104 *2.2. Culturing fruit cuts on MS medium supplemented with [1-^{13}C]sorbitol*

105 Within 2 h after the collection, an above-mentioned apple fruit was surface sterilized
106 by dipping it in 70% ethanol for 30 sec, then in sodium hypochlorite solution
107 (approximately 1% active chlorine) for 15 min, and rinsed 3 times with sterilized
108 distilled-deionized water. At first, the fruit was cut vertically along with the central axis
109 on a sterilized Kim towel spread in a laminar air-flow cabinet. Then, a piece of the cut
110 fruit was cut vertically again along with the central axis, and another piece was cut
111 horizontally at the maximum width of the ovary cell, respectively. One of the final
112 pieces of both the longitudinal and horizontal cuttings was cultured on an
113 agar-solidified Murashige and Skoog (MS) medium (pH 5.7) supplemented with 0.5 M
114 [1-^{13}C]sorbitol at 25˚C for 72 h under 16 h daily illumination (60 μmol/m^2/s, daylight
115 LED). In this case, the medium (0.7% agar was dissolved by boiling) was autoclaved at
116 121˚C, 1.1 kg/cm^2 for 15 min, and then dispensed into a petri-dish (50 mm in diameter)
117 in a laminar air-flow cabinet. The concentration (0.5 M) of [1-^{13}C]sorbitol was decided

118 by considering the total molar concentration (calculated as 0.48 M) of soluble
119 carbohydrates in juice from the mature apple fruits (Fuleki et al., 1994). The quarter
120 cuts of the fruit were stood on the medium in the petri-dish with the cut face being
121 attached fully to the medium (Fig. 2), covered with a lid and sealed with Parafilm. The
122 cultured fruit cut, and another piece of fruit cut which had the same cut face (opposite)
123 were both stored at -80˚C until preparing the specimens.
124
125 *2.3. Preparation of apple fruit specimens*
126 Thin (100 µm) longitudinal and horizontal flesh specimens of both the cultured and
127 non-cultured cuts were sliced on a cryo-microtome (CM3050S, Leica Biosystems
128 Nussloch GmbH, Nussloch, Germany) at just inside of the cut face (Suppl. 1). The
129 specimen was mounted on an indium tin oxide (ITO) coated glass slide (#8237001,
130 Bruker Daltonics GmbH & Co. KG, Bremen, Germany), quickly lyophilized and
131 stored at -30˚C.
132
133 *2.4. HPLC*
134 Three different fruits collected on the same day were cut similarly, and a piece of
135 each fruit cut, longitudinally or horizontally, was cultured on an agar-solidified MS
136 medium (pH 5.7) supplemented with 0.5 M of naturally occurred sorbitol. Vertical and
137 horizontal thin (100 µm) specimens from both the cultured fruit cut and another fruit
138 cut having the opposite cut face (before culturing) were sliced on a cryo-microtome in
139 the same manner as mentioned above. Two serial specimens (around 240 mg in total
140 fresh weight) from in each fruit cut were extracted with 2 mL of 80%(v/v) ethanol at
141 70˚C in a water bath for 30 min, supplemented with 1 mL of 20 mM lactose as an
142 internal standard, homogenized in a mortar with pestle, and centrifuged at 14,000 × *g*
143 for 5 min. The supernatant was concentrated to approximately 0.5 mL using a

centrifuge evaporator, then centrifuged at 14,000 × *g* for 5 min prior to analysis of carbohydrates. Water content was determined by drying specimens at 70˚C for 3 days before culturing in a drying oven and then expressed as a percentage of fresh weight (FW). Levels of carbohydrates in the supernatant were determined by HPLC, according to the method reported previously (Horikawa et al., 2019). The conditions for HPLC were as follows: mobile phase, 75%(v/v) acetonitrile; pump (L-6200; Hitachi, Tokyo, Japan); column (NH2P-50 4E; Shodex, Tokyo, Japan); detector, refract intensity (RI)-monitor (L-3300; Hitachi); temperature, 30˚C (L-5020 column oven; Hitachi); flow rate, 0.7 mL/min; and sample volume, 10 μL.

2.5. MALDI–TOF MSI

MALDI–TOF MSI analysis of the apple fruit specimen previously sprayed with a solution of 5 %(w/v) DHB in 70%(v/v) methanol, 1 mL for a glass slide, applied using an airbrush (CHMX6011-1; Anest Iwata Corp., Yokohama, Japan) was performed by a MALDI–TOF MS instrument (ultrafleXtreme, Bruker Daltonics) equipped with a Nd:YAG laser (355 nm) producing 0.5 ns pulses with the repetition rate set to 1000 Hz, with an accelerating voltage of 20 kV and the reflector positive-ion mode with delayed extraction at 280 ns. All mass spectra were generated by collecting 500 laser shots and *m/z* values were calibrated with the ion peak of cesium iodide loaded on the slide (outside of the specimen). The interval of the probing spots on the specimen was set at 400 μm. An optical image of the distribution of independent carbohydrate was constructed using flexImaging v4.0 (Bruker Daltonics) upon acquired mass spectra at every MSI grid array coordinate.

2.6. Statistical analysis of data

169 The content of carbohydrates was represented as mean ± SE (n = 3). The difference
170 between the content of carbohydrates in cultured specimens and that before culturing
171 was analyzed statistically by Student's t-test.
172
173 **3. Results and discussion**
174 There are three reasons why we used young fruits at their developing stage collected
175 in late July as plant material in the present study. The first is that it was difficult to
176 obtain intact specimens on a cryo-microtome by slicing a half-sized dimension of
177 mature fruit flesh because the flesh was composed of relatively large cells with large
178 intercellular space (Suzuki et al., 2003). The second is that this was the maximum fruit
179 size that could be used as specimens and mounted on a normal-sized ITO glass slide,
180 even with 'Kotoku', which has a relatively small fruit size. The third is that since the
181 concentration of soluble carbohydrates in the mature fruits was high, we thought that
182 high osmolarity in the flesh of mature fruits would disturb penetration of external
183 sorbitol into the tissue, which would make it hard to track the changes in content of
184 soluble carbohydrates.
185 The content of soluble carbohydrates in the fruit flesh specimen obtained from the
186 fruit cut with or without culturing for 72 h on the sorbitol rich medium is shown in Fig.
187 3. The mean value (mg/gFW) of those from the longitudinal and horizontal specimens
188 before culturing was as follows: sorbitol, 3.4; glucose, 8.0; fructose, 25.6; sucrose, 15.0.
189 Since the water (%) of the specimens before culturing was 85.6 ± 0.2 (mean ± SE, n =
190 6), they could be converted into the following values (g/L): sorbitol, 4.0; glucose, 9.3;
191 fructose, 29.9; sucrose, 17.5. Furthermore, total molar concentration of soluble
192 carbohydrates in the tissue was calculated as 0.29 M, which was lower than the sorbitol
193 concentration (0.5 M) added to the medium. As a result, sorbitol penetrated gradually
194 into the flesh tissue to keep osmotic equivalence (Suzuki et al., 1997). Li et al. (2012)

showed similar values (mg/gFW) on ‘Greensleeves’ apple fruits collected 74 days after bloom: sorbitol, 5; glucose, 5; fructose, 48; sucrose, 18. On the other hand, Fuleki et al. (1994) reported that the concentration (g/L) of sorbitol, glucose, fructose and sucrose was 2.8, 13.3, 54.0 and 32.5 in juice obtained from mature fruits of 11 apple cultivars. Thus, the content of glucose, fructose and sucrose in the young apple fruits 75 days after bloom used in the present study seems lower (54–70%) than that of the mature fruits, even though the content of sorbitol showed similar values. Furthermore, since sorbitol content in the specimens from the cultured fruit cuts was 4.9–5.7 times greater ($P < 0.01$) than the content before culturing in both longitudinal and horizontal sections, it could be that external sorbitol was taken up by the tissue of the fruit cuts during the culture. The content of glucose and fructose in the specimens from the cultured fruit cuts showed 2.0–2.2 and 1.2–1.4 times greater values ($P < 0.05$ and $P < 0.01$, respectively) than those before culturing. By contrast, the sucrose content in the specimens from the cultured fruit cuts showed approximately half the values ($P < 0.01$) of those before culturing. The decrease in sucrose content indicates that activity of the sucrose degradation by invertase was stronger than that of the sucrose biosynthesis in the cultured fruit tissues. Actually, Li et al. (2012) showed that the activity of SDH, neutral invertase and SuSy was higher, but that of SPS was lower in young (74 days after bloom) fruits than in mature (134 days after bloom) fruits. Thus, the increase in the hexose content seems to be caused not only by biosynthesis from sorbitol but by degradation of sucrose.

On the MALDI-TOF MSI, an example mass spectrum of the apple fruit specimen from the fruit cut with or without culturing on the [1-^{13}C]sorbitol supplemented medium were shown in Fig. 4. Three peaks having *m/z* 219.0, 221.0 and 381.1 were found in those mass spectra, and they were identified as naturally occurred hexose, sorbitol and sucrose attached with a potassium ion, since the values were the same as those shown

by Horikawa et al. (2019). The hexose peak was originated from glucose and fructose, but since ion intensity of fructose was approximately 6-fold greater than that of glucose at the same concentration when DHB was used as a matrix (Horikawa et al., 2019), and furthermore the concentration of fructose in the specimen was approximately two times higher than that of glucose (Fig. 3), the distribution of hexose constructed by MSI might depend mainly on fructose. Peaks having *m/z* 220.0, 222.0, 382.1 and 383.1 could also be found in the mass spectra. Since the abundance ratio of the 222.0 peak, calculated as the height of the 222.0 peak/height of the 221.0 (naturally occurred sorbitol) peak ×100 (%), in the specimen cultured with [1-^{13}C]sorbitol was greater than the abundance ratio (1.1%) of the natural ^{13}C, it could be that the peak of *m/z* 222.0 represents [^{13}C-Sor + K]$^+$ which was originated from external [1-^{13}C]sorbitol that penetrated into the tissue. Similarly, the peaks of *m/z* 220.0, 382.1 and 383.1 would represent ([Hex + K]$^+$ + 1), ([Suc + K]$^+$ + 1) and ([Suc + K]$^+$ + 2) respectively, which were biosynthesized from the substrate [1-^{13}C]sorbitol in the tissue during the culture (Fig. 5).

Heat map images on the distribution of the peaks of [^{13}C-Sor + K]$^+$, ([Hex + K]$^+$ + 1), [Suc + K]$^+$, ([Suc + K]$^+$ + 1) and ([Suc + K]$^+$ + 2) in specimens before and after the culture constructed by MALDI–TOF MSI are shown in Fig. 6. During the culture of fruit cuts, uneven penetration of sorbitol into the flesh tissue might have occurred, which would affect the results of MSI. To avoid this, we used specimens just inside the cut face. As a result, high densities and even distribution of [^{13}C-Sor + K]$^+$ peaks were observed on the specimens cultured with [1-^{13}C]sorbitol regardless of the way it was cut, when being compared with uncultured specimens, and furthermore with those of naturally occurred (^{12}C) sorbitol (Suppl. 2). These facts indicate that external [1-^{13}C]sorbitol added to the medium had penetrated evenly into the tissue close to the cut face. Densities of ([Hex + K]$^+$ + 1) were also higher in the cultured specimens than those before culturing, and no gradation could be found in the distribution of hexose.

247 The hexose containing a ^{13}C-atom could be biosynthesized from external [1-^{13}C]sorbitol
248 in the cultured tissue. However, hexose distribution constructed by MSI seems
249 unreliable since it was originated from both glucose and fructose molecules, which had
250 a different ion intensity at a same concentration, and furthermore which might have a
251 different distribution pattern in the tissue. On the peaks of ([Suc + K]$^+$ + 1) and ([Suc +
252 K]$^+$ + 2), since abundance was also stronger in the cultured specimens, sucrose
253 molecules containing 1 or 2 of ^{13}C-atoms could be biosynthesized from external
254 [1-^{13}C]sorbitol via hexose in the cultured tissue, even though degradation of sucrose
255 was greater than biosynthesis. Furthermore, graded distribution of sucrose containing
256 ^{13}C in a molecule was confirmed from the center to the outer areas of the fruit. There
257 tended to be a higher abundance at the cortex side, lower at the pith side, and quite low
258 near the pedicel. Low abundance near the pedicel might be caused by sucrose
259 degradation, since the abundance of the naturally occurred sucrose ([Suc + K]$^+$) had
260 decreased at this region after the culture. However, no graded distribution of naturally
261 occurred sucrose was observed in the cultured fruit flesh. These facts indicate that
262 sucrose biosynthesis might be active at the cortex side of the receptacle in the cultured
263 fruit cuts. On this point, since SPS activity of the young fruits (74 days after bloom) was
264 low (Li et al., 2012), and no graded distribution of ^{12}C-sucrose was observed in the
265 specimens before culturing (Fig. 6), sucrose biosynthesis might be driven by external
266 sorbitol accumulated in the tissue via the activated kinase SnRK1 (Yu et al., 2020). In
267 other words, potential ability of biosynthesizing sucrose would be high at tissue around
268 the cortex, especially at the peripheral regions of the fruits, which may lead to the
269 graded increase in sucrose concentration from the center to the outer areas of the mature
270 apple fruits. To clarify the cause of graded sucrose distribution, enzymatic activities on
271 sucrose biosynthesis or functions of sorbitol transporter should be compared between
272 the inner and outer regions of receptacle tissue. Furthermore, this graded distribution of

sucrose might be a signal for inducing ripening of fruits (Jia et al., 2013), resulting in anthocyanin accumulation into the epidermis and formation of volatile components.

4. Conclusions

In the present study, a quarter cut of young apple fruit, with a longitudinal or horizontal cut face, was cultured with 0.5 M [1-^{13}C]sorbitol as a substrate, and then distribution of ^{13}C-labelled sucrose biosynthesized *in vitro* in a cultured tissue was visualized using MALDI-TOF MSI. Heatmap images showed external [1-^{13}C]sorbitol had penetrated evenly into the tissue. Furthermore, a graded increase in ^{13}C-labelled sucrose was observed from center to outer of the fruit. Thus, it was concluded that sucrose biosynthetic ability might be higher at the cortex side of the receptacle than at the pith side in the apple fruit flesh tissue. The method utilizing MALDI-TOF MSI combined with the treatment of a stable isotope-labelled substrate would be useful for visualizing biosynthetic reactions of phytochemicals in a plant tissue, and available in such a case as breeding new apple cultivars having unique taste.

Acknowledgements

The authors thank Mr. Minoru Ikuta, a technical staff at experimental farm in Hokkaido University, for growing ‘Kotoku’ apple trees in the Yoichi orchard with excellent management skills.

Funding

This work was supported by Japan Society for the Promotion of Science (JSPS KAKENHI Grant Number JP21H02180).

CRediT authorship contribution statement

Ruka Yamashita: Methodology, Formal analysis, Investigation, Resources, Data curation, Writing – original draft, Visualization. **Takumi Fujiki**: Investigation, Data curation. **Kentaro Horikawa**: Methodology. **Yutaka Jitsuyama**: Data curation, Funding acquisition. **Jun Kasuga**: Data curation, Funding acquisition. **Keiji Ueno**: Data curation, Funding acquisition. **Takashi Suzuki**: Conceptualization, Data curation, Formal analysis, Funding acquisition, Investigation, Methodology, Project administration, Resources, Supervision, Validation, Visualization, Writing – review & editing.

Declaration of competing interest

All authors declare that they have no conflict of interest.

Data availability

Data will be made available on request.

Appendix A. Supplementary data

Supplementary data to this article can be found on line at https://www2.cloud.editorialmanager.com/foodchem/download.aspx?id=5168710&guid=5472ff27-5f0b-46d3-94d1-dc364c98288e&scheme=1

References

Aprea, E., Charles, M., Endrizzi, I., Corollaro, M.L., Betta, E., Biasioli, F., & Gasperi, F. (2017). Sweet taste in apple: the role of sorbitol, individual sugars, organic acids and volatile compounds. *Scientific Reports, 7*, 44950. https://doi.org/10.1038/srep44950

Enomoto, H., Sato, K., Miyamoto, K., Ohtsuka, A., & Yamane, H. (2018). Distribution analysis of anthocyanins, sugars, and organic acids in strawberry fruits using Matrix-Assisted Laser Desorption/Ionization-Imaging mass spectrometry. *Journal of Agricultural and Food Chemistry, 66*, 4958–4965. https://doi.org/10.1021/acs.jafc.8b00853

Feenstra, A.D., Dueñas, M.E., & Lee, Y.J. (2017). Five micron high resolution MALDI mass spectrometry imaging with simple, interchangeable, multi-resolution optical system. *Journal of the American Society for Mass Spectrometry, 28*, 434–442. https://doi.org/10.1007/s13361-016-1577-8

Franceschi, P., Dong, Y., Strupat, K., Vrhovsek, U., & Mattivi, F. (2012). Combining intensity correlation analysis and MALDI imaging to study the distribution of flavonols and dihydrochalcones in Golden Delicious apples, *Journal of Experimental Botany, 63*, 1123–1133. https://doi.org/10.1093/jxb/err327

Fujita, R., Hayasaka, T., Jin, S., Hui, S., & Hoshino, Y. (2019). Comparison of anthocyanin distribution in berries of Haskap (*Lonicera caerulea* subsp. *edulis* (Turcz. ex. Herder) Hultén), Miyama-uguisukagura (*Lonicera gracilipes* Miq.), and their interspecific hybrid using imaging mass spectrometry, *Plant Science, 278*, 110633. https://doi.org/10.1016/j.plantsci.2020.110633

Fuleki, T., Pelayo, E., & Palabay, R.B. (1994). Sugar composition of varietal juices produced from flesh and stored apples, *Journal of Agricultural and Food Chemistry, 42*, 1266–1275. https://doi.org/10.1021/jf00042a003

Gao, Z., Jayanty, S., Beaudry, R., & Loescher, W. (2005). Sorbitol transporter expression in apple sink tissues: implications for fruit sugar accumulation and watercore development, *Journal of the American Society for Horticultural Science, 130*, 261–268. https://doi.org/10.21273/JASHS.130.2.261

Horikawa, K., Hirama, T., Shimura, H., Jitsuyama, Y., & Suzuki, T. (2019). Visualization of soluble carbohydrate distribution in apple fruit flesh utilizing MALDI–TOF MS imaging, *Plant Science, 278*, 107–112. https://doi.org/10.1016/j.plantsci.2018.08.014

Jia, H., Wang, Y., Sun, M., Li, B., Han, Y., Zhao, Y., Li, X., Ding, N., Li, C., Ji, W., & Jia, W. (2013). Sucrose functions as a signal involved in the regulation of strawberry fruit development and ripening, *New Phytologist, 198*, 453–465. https://doi.org/10.1111/nph.12176

Kaspar, S., Peukert, M., Svatos, A., Matros, A., & Mock, H. (2011). MALDI–imaging mass spectrometry – an emerging technique in plant biology. *Proteomics, 11*, 1840–1850. http://doi.org/10.1002/pmic.201000756

Li, M., Feng, F., & Cheng, L. (2012). Expression patterns of genes involved in sugar metabolism and accumulation during apple fruit development, *PLoS ONE, 7*, e33055. http://doi.org/10.1371/journal.pone.0033055

Li, M., Li, P., Ma, F., Dandekar, A.M., & Cheng, L. (2018). Sugar metabolism and accumulation in the fruit of transgenic apple trees with decreased sorbitol synthesis, *Horticulture Research, 5*, 60. https://doi.org/10.1038/s41438-018-0064-8

Loescher, W.H., Marlow, G.C., & Kennedy, R.A. (1982). Sorbitol metabolism and sink-source interconversions in developing apple leaves, *Plant Physiology, 70*, 335–339. https://doi.org/10.1104/pp.70.2.335

Lu, D., Wu, Y., Zhang, J., Qi, Y., Zhang, Y., & Pan, Q. (2023). Visualizing the distribution of jujube metabolites at different maturity stages using Matrix-Assisted Laser Desorption/Ionization Mass Spectrometry Imaging. *Foods, 12*, 3795. https://doi.org/10.3390/foods12203795

374 Nakanishi, T., Takai, S., Jin, D., & Takubo, T. (2013). Quantification of candesartan in
375 mouse plasma by MALDI-TOF MS and in tissue sections by MALDI-imaging
376 using the stable-isotope dilution technique, *Mass Spectrometry, 2*, A0021.
377 https://doi.org/10.5702/massspectrometry.A0021
378 Sha, J., Wang, F., Xu, X., Chen, Q., Zhu, Z., Jiang, Y., & Ge, S. (2020). Studies on the
379 translocation characteristics of ^{13}C-photoassimilates to fruit during the fruit
380 development stage in 'Fuji' apple, *Plant Physiology and Biochemistry, 154*,
381 636–645. https://doi.org/10.1016/j.plaphy.2020.06.044
382 Suzuki, T., Kaneko, M., & Harada, T. (1997). Increase in freezing resistance of excised
383 shoot tips of *Asparagus officinalis* L. by preculture on sugar-rich media,
384 *Cryobiology, 34*, 264-275. https://doi.org/10.1006/cryo.1997.2004
385 Suzuki, T., Maeda, T., Grant, S., Grant, G., & Sporns, P. (2013). Confirmation of
386 fructans biosynthesized in vitro from [1-^{13}C]glucose in asparagus tissues using
387 MALDI–TOF MS and ESI–MS, *Journal of Plant Physiology, 170*, 715–722.
388 https://doi.org/10.1016/j.jplph.2012.12.005
389 Suzuki, T., Sasaki, Y., Kuroda, K., & Oosawa, K. (2003). Histological features and
390 dynamics of the development of water core in apple (*Malus domestica*) fruit. *Acta*
391 *Horticulturae, 628*, 495-500. https://doi.org/10.17660/ActaHortic.2003.628.61
392 Wang, J., Yang, E., Chaurand, P., & Raghavan, V. (2021). Visualizing the distribution
393 of strawberry plant metabolites at different maturity stages by MALDI-TOF
394 imaging mass spectrometry. *Food Chemistry, 345*, 128838.
395 https://doi.org/10.1016/j.foodchem.2020.128838
396 Yamaki, S. (1984). $NADP^+$–dependent sorbitol dehydrogenase found in apple leaves,
397 *Plant and Cell Physiology, 25*, 1323–1327.
398 https://.doi.org/10.1093/oxfordjournals.pcp.a076843

399 Yamaki, S. (2010). Metabolism and Accumulation of Sugars Translocated to Fruit and
400 Their Regulation, *Journal of the Japanese Society for Horticultural Science, 79*,
401 1–15. https://doi.org/10.2503/jjshs1.79.1
402 Yamaki, S., & Ishikawa, K. (1986). Roles of four sorbitol related enzymes and
403 invertase in the seasonal alteration of sugar metabolism in apple tissue, *Journal of*
404 *the American Society for Horticultural Science, 111*, 134-137.
405 https://doi.org/10.21273/JASHS.111.1.134
406 Yoshimura, Y., Enomoto, H., Moriyama, T., Kawamura, Y., Setou, M., & Zaima, N.
407 (2012). Visualization of anthocyanin species in rabbiteye blueberry *Vaccinium*
408 *ashei* by matrix-assisted laser desorption/ionization imaging mass spectrometry,
409 *Analytical and Bioanalytical Chemistry, 403*, 1885–1895.
410 https://doi.org/10.1007/s00216-012-5876-z
411 Yu, W., Peng, F., Wang, W., Liang, J., Xiao, Y. & Yuan, X. (2020). SnRK1
412 phosphorylation of SDH positively regulates sorbitol metabolism and promotes
413 sugar accumulation in peach fruit, *Tree Physiol*ogy, 41, 1077–1086.
414 https://doi.org/10.1093/treephys/tpaa163
415 Yuan, J., Wang, Z., Wang, X., Zhang, C., Ma, F., & Li, M. (2023). Research advances
416 in genetic quality of sugar content in apples. *Fruit Research, 3*, 13.
417 https://doi.org/10.48130/FruRes-2023-0013
418
419
420 **Legend of Figures**
421 **Fig. 1.** A simple scheme on pathways related to biosynthesis and degradation of
422 sucrose in apple fruit.
423

Fig. 2. A scheme of culturing cut fruits on MS medium supplemented with [1-^{13}C]sorbitol.

Fig. 3. Content of soluble carbohydrates in longitudinal and horizontal specimens from apple fruit flesh before (white bar) and after (dark bar) culturing *in vitro* for 72 h on MS medium supplemented with 0.5 M sorbitol. Sor, sorbitol; Glc, glucose; Fru, fructose; Suc, sucrose. Data represent mean ± SE (n = 3). $^{***}P < 0.001$, $^{**}P < 0.01$ and $^{*}P < 0.05$ (Student's t-test).

Fig. 4. Example MALDI–TOF mass spectra of the apple fruit specimen from a fruit cuts cultured on MS medium supplemented with or without 0.5 M [1-^{13}C]sorbitol.

Fig. 5. Possible combinations of glucose and fructose molecule(s) in terms of the number of ^{13}C in sucrose which had 1 or 2 m/z heavier values (the 382.1 m/z, the 383.1 m/z) than expected values on MALDI–TOF mass spectra shown in Fig. 4. Digits on the figures of sorbitol, glucose and fructose molecules represent the number of ^{13}C-atoms possessed. Squares with broken lines show combinations of sucrose molecules with a ^{13}C-atom. Sor, sorbitol; Glc, glucose; Fru, fructose.

Fig. 6. Heat map images constructed by MALDI–TOF MSI on the distribution of carbohydrates containing one or two ^{13}C-atoms in a molecule and naturally occurred (^{12}C) sucrose in longitudinal and horizontal specimens before and after culturing 72 h on MS medium supplemented with 0.5 M [1-^{13}C]sorbitol. Sor, sorbitol; Hex, hexose; Suc, sucrose. White bars represent 1 cm in length. On the heat map scale of 0–100%, graded color represents the peak height ratio (%) of a spot to the highest peak (100%) of each molecular ion at every MSI grid array coordinate.

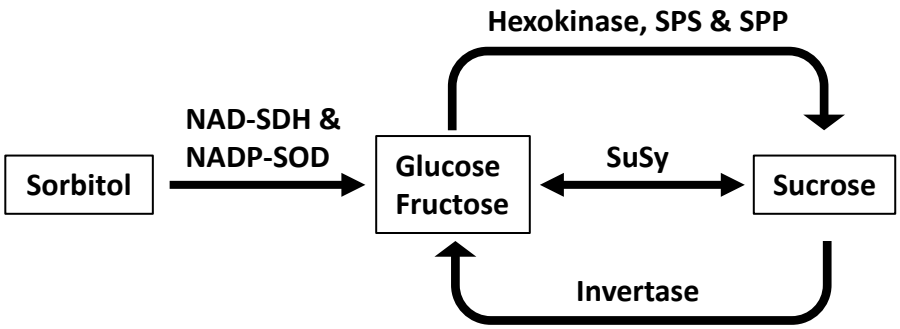
Hexokinase, SPS & SPP
NAD-SDH &
NADP-SOD
Sorbitol
Glucose
Fructose
SuSy
Sucrose
Invertase

Fig. 1

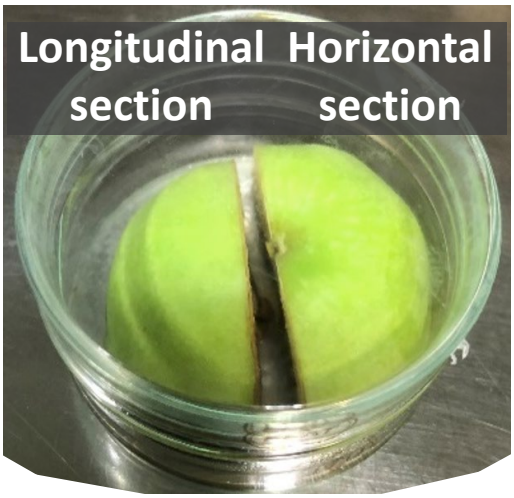

Agar solidified MS medium + 0.5 M [1-^{13}C]sorbitol

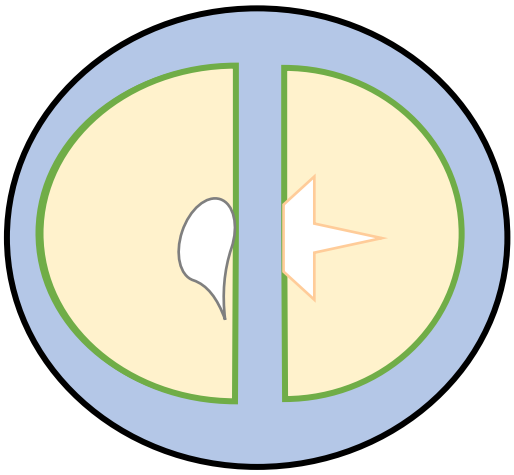

View from the bottom of Petri-dish

Fig. 2

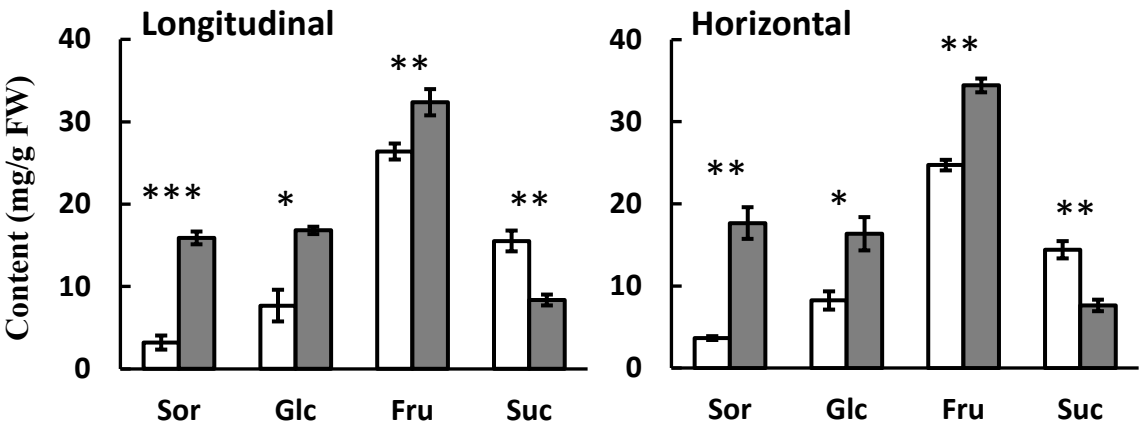
Longitudinal
Horizontal
Content (mg/g FW)
40
30
20
10
0
***
*
**
**
**
*
**
**
Sor
Glc
Fru
Suc
Sor
Glc
Fru
Suc

Fig. 3

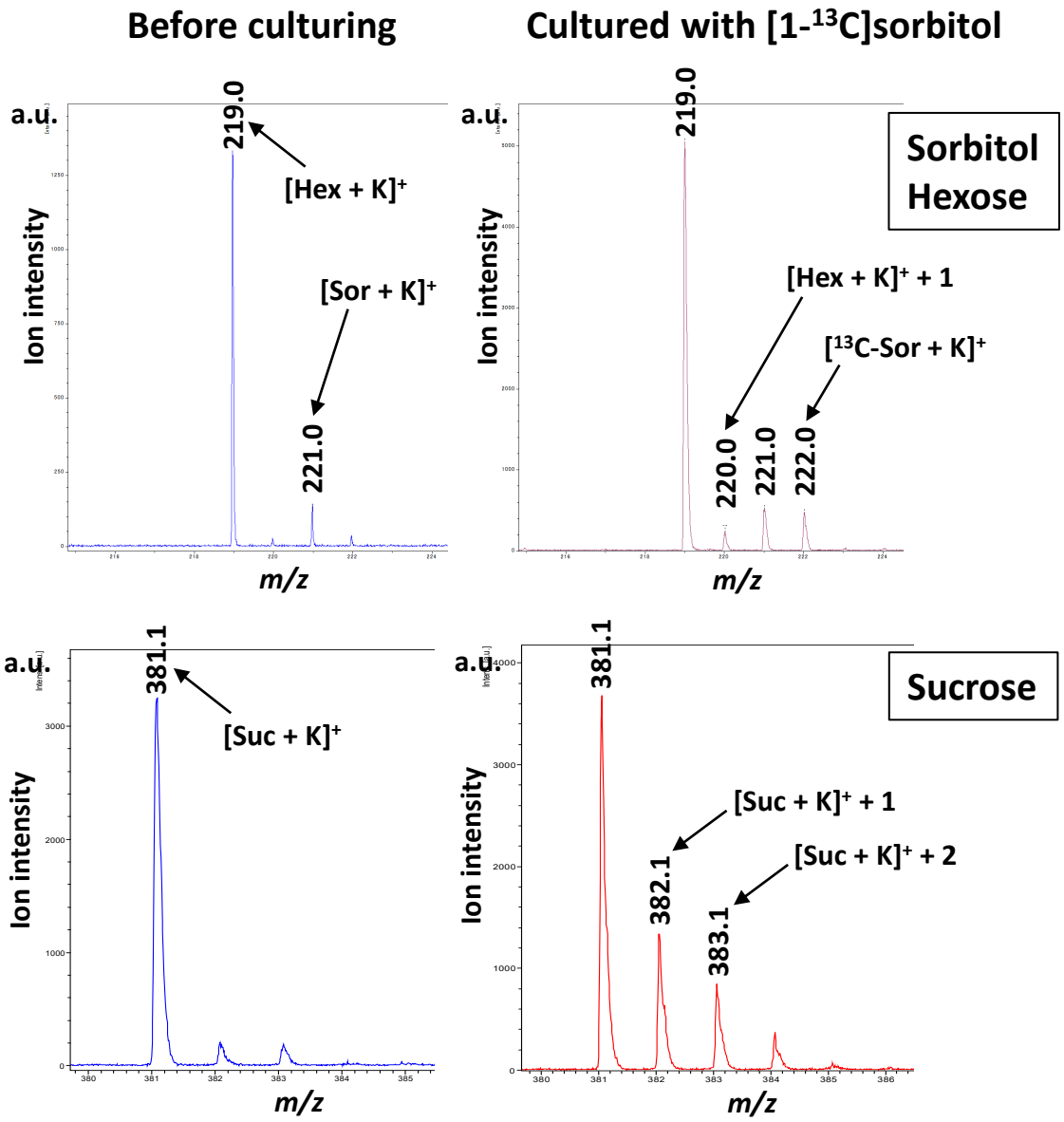
Before culturing
Cultured with [1-13C]sorbitol
a.u.
Ion intensity
219.0
[Hex + K]+
[Sor + K]+
221.0
m/z
Sorbitol
Hexose
[Hex + K]+ + 1
[13C-Sor + K]+
220.0
221.0
222.0
381.1
[Suc + K]+
Sucrose
[Suc + K]+ + 1
[Suc + K]+ + 2
382.1
383.1

Fig. 4

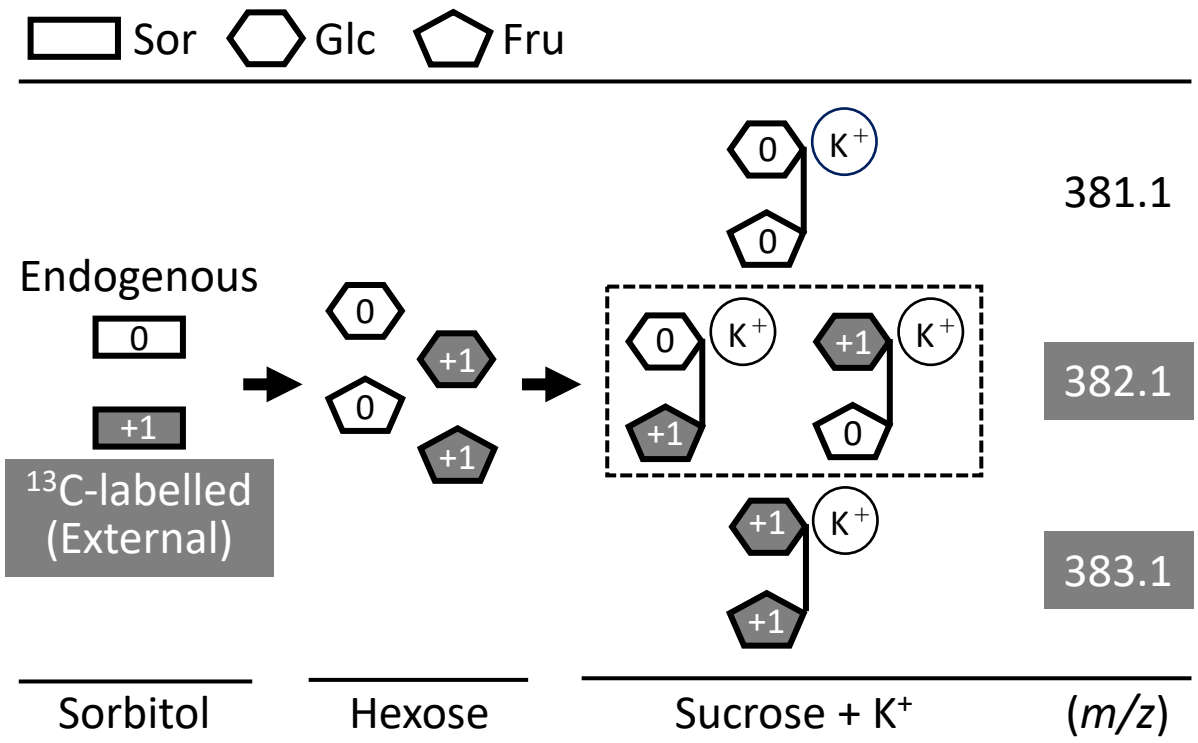
Sor
Glc
Fru
Endogenous
0
+1
13C-labelled
(External)
0
0
+1
+1
0
K+
0
+1
K+
+1
0
K+
+1
+1
381.1
382.1
383.1
Sorbitol
Hexose
Sucrose + K+
(m/z)

Fig. 5

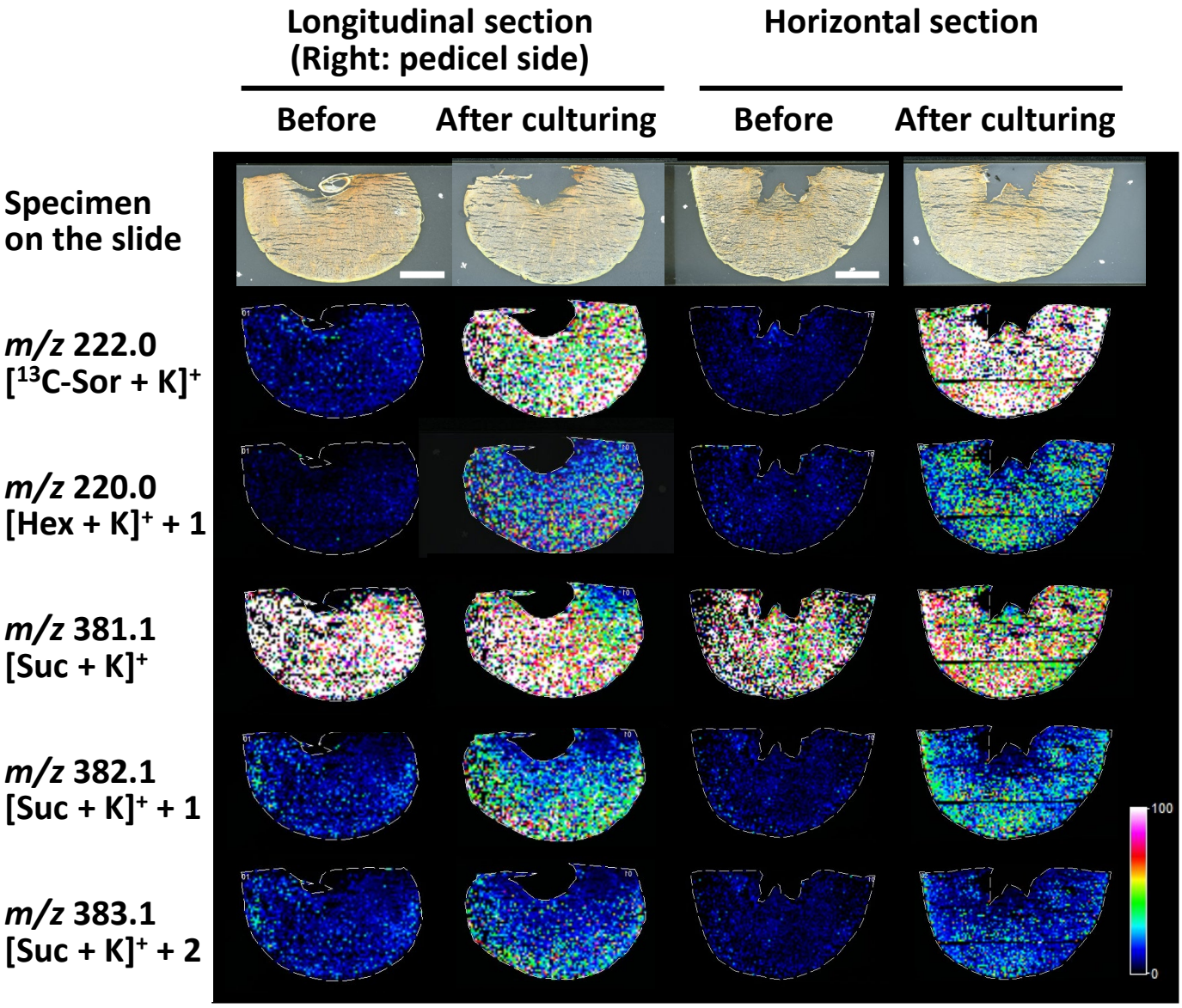
Longitudinal section
(Right: pedicel side)
Horizontal section
Before
After culturing
Before
After culturing
Specimen on the slide
m/z 222.0
[13C-Sor + K]+
m/z 220.0
[Hex + K]+ + 1
m/z 381.1
[Suc + K]+
m/z 382.1
[Suc + K]+ + 1
m/z 383.1
[Suc + K]+ + 2
100
0

Fig. 6